Semiconductor Physics, Quantum Electronics & Optoelectronics, 2017. V. 20, N 3. P. 375-381.

PACS 73.61.Ey, 77.22.Gm, 82.75.-z, 84.37.+q

The influence of the guest cavitations loading degree in fractal nanohybrids GaSe⟨β-cyclodextrin⟨$FeSO_4$⟩⟩ on the current passing and polarization processes. The giant "battery spin" effect at room temperature.

F.O. Ivashchyshyn[1], I.I. Grygorchak[1], O.I. Hryhorchak[2]
[1]*Lviv Polytechnic National University, 12, Bandera Str., Lviv 79013, Ukraine*
[2]*Ivan Franko National University of Lviv, 8, Kyrylo and Mefodiy str., 79005 Lviv, Ukraine*

Abstract. The investigation results of clathrate properties GaSe⟨β-cyclodextrin⟨$FeSO_4$⟩⟩ of the hierarchical architecture with the fourfold expansion at different degrees of a guest cavitations loading have been presented. Based on the frequency dependence of the specific complex impedance, the changes of the impurity energy spectrum expanded matrix parameters as a result of forming the supramolecular ensembles on its basis are clarified. For some architecture, impedance, photo and magneto responses showed the extraordinary behavior of the magnetoimpedance and photoconductivity and also the giant negative photodielectric and the colossal magnetocapacitance effects at room temperature, which open new possibilities of their practical application.

Keywords: layered semiconductor GaSe, β-cyclodextrin, "host-guest" system, hierarchical architecture, impedance, Nyquist's diagram, dielectric constant, tangent of angle of electric losses, photodielectric effect, magnetocapacity, "battery-spin" effect.

Manuscript received 23.05.17; revised version received 00.00.17; accepted for publication 00.00.17; published online 00.00.17.

1. Introduction

Like to other semiconductor materials, deep defect states in the band gap of InGaAs are formed by doping with a wide class of impurities [5]. These states may be significantly complicated due to formation of dopant pairs or their interaction with their own lattice defects. Optical and electronic properties are studied by photocurrent (PC) spectra and thermal activation effects measurement [3]. However, thermally stimulated conductivity (TSC) spectra of InGaAs-GaAs hetero-structures with QW are not examined enough. According to [1-3], distribution of localized states in semiconductors is based on the multiple trapping model. It was shown that peaks in the spectra TSC were observed within the Despite the rapid development of the supramolecular chemistry in the recent decade, there are significantly a few publications aimed to studying the physical properties of supramolecular architectures and clathrates. Their analysis allowed concluding that the research results of semiconductor clathrates as phonon glasses, the most promising thermoelectric materials, are the closest ones to practical application. The solution of the Slack hypothesis [1, 2] about formation of these structures, in which the weakly bound atoms can oscillate in a limited volume and provide a low thermal conductivity at high electrical conductivity, is almost found [3]. As for the other physical aspects of "host-guest" supramolecular ensembles, at first the papers devoted to the electronic structure calculations (see, *e.g.*, [4]) or the systems with excitation energy transfer [5] should be emphasized.

Recently, we [6] have synthesized the supramolecular ensemble of a fundamentally new architecture as subhost⟨host⟨guest⟩⟩, where the organic/inorganic cavitate β-cyclodextrin (β-CD), and ferrous sulphate serve as a guest content in the inorganic MCM-41 SiO_2-submatrix, forming the guest hierarchy in this way. The colossal magneto capacitance effect and the huge (almost tenfold) alternative-current (in the $10^3 \ldots 10^6$ Hz frequency range) negative magneto resistance effect were detected in this supramolecular

ensemble at room temperature and weak magnetic fields for the first time. These extraordinary properties of hierarchical clathrates definitely actualize the further research development, especially studying the dependence of the physical processes passing on the subhost matrix type and also clarifying the influence of the cavitation loading degree on them. This paper is devoted to these issues.

2. Conceptual fundamentals and methodology of experiments

Taking into account the increasing interest to the nanophotoelectronics and quantum coherent spintronics, the set goal was achieved by replacing the molecular-lattice dielectric SiO_2-subhost with the photosensitive quasi-2D semiconductor of gallium selenide (GaSe). On its basis the clathrates with hierarchical architecture of GaSe⟨β-CD⟨$FeSO_4$⟩⟩ formed by the host contents cavitation on a "host-guest" type were synthesized.

Single crystals GaSe grown with the Bridgman–Stockbarger method had a brightly expressed layered structure and *p*-type conductivity. The band gap (due to the optical data) was 2.02 eV. It is well known [7] that they are characterized by the presence of the so-called "guest" positions oriented perpendicularly to crystallographic axis *C* of the areas of weak van der Waals forces. Inclusion of foreign ions, atoms or molecules into the appointed intracrystalline intervals is known as an intercalation phenomenon [8]. The absence of dangling bonds on the surfaces provides a very low surface recombination velocity. In addition, these single crystals are highly photosensitive in a visible spectrum.

The organic cavitand, such as cyclodextrin of β-form (β-CD), was used as an intermediate host. Its unique structural feature, namely separation of hydrophilic and hydrophobic groups, causes unusual physical and chemical properties. The most important among them is the ability of the selective and backward binding of organic, inorganic, biological molecules, forming the complexes of inclusions with the "key-lock" type in this way. The large electron density inside the cavity of β-CD can activate electrons of molecules of "guests", which leads to the changes in the spectral properties of the included molecules as well as the β-CD [9]. Iron (II) sulfate served as a substrate, which is known precursor for the synthesis of nanomagnetite, which cationic component has a large spin magnetic moment.

Since neither β-cyclodextrin nor ferrous sulfate are implemented into GaSe directly, the three-stage intercalation-deintercalation technology described in details in our paper [10] was used to form the supramolecular ensembles, and as a result the fourfold output matrix expansion degree was achieved. The cavitate content increases in the extended GaSe matrixes was achieved by the step-by-step intercalation of the samples. The precise gravimetric and chemical analyses were made at each stage.

The impedance measurements were made in the direction of crystallographic axis C in the 10^{-3}…10^{6} Hz frequency range by using the measuring complex "AUTOLAB" of "ECO CHEMIE" (Holland), which is equipped with computer software FRA-2 and GPES. Removing the questionable points was made with Dirichlet's filter [10, 11]. The frequency dependences of complex impedance (Z) were analyzed using the graphic-analytical method in the software package ZView 2.3 (Scribner Associates). Approximation errors did not exceed 4%. The adequacy of the impedance models built on the basis of the experimental data group was confirmed completely by the random nature of frequency dependences of the first-order remaining differences [11, 12]. The investigated samples were lightened with the visible light or the constant magnetic field perpendicular to the nanolayers of 2.75 kOe tension was applied to them.

3. The results and discussion

Fig. 1 shows the frequency dependences of the real component of the complex specific impedance (Re $Z(\omega)$) perpendicular to the nanolayers planes of the fourfold extended GaSe, before and after implementing the different amounts of cavitate β-CD ⟨$FeSO_4$⟩. It is seen that, at the room temperature (293 K), Re $Z(\omega)$ for the initial extended matrix GaSe behaves as usual: the quasi-horisontal infra low-frequency branch moves to the declining one at higher frequencies, because of contribution of charge carriers hopping on the localized states at the Fermi level or the processes of exciting-capturing them in the zones tails (or the delocalized states zones) [13, 14]. The first inclusion of β-CD⟨$FeSO_4$⟩ (curve *2*) causes to over 20-fold reduction of Re $Z(\omega)$ in the mentioned range, mainly because of the delocalized (zone) carriers. With further increasing the amount of the guest cavitate loading (Q) in van der Waals enhanced areas of GaSe, Re $Z(\omega)$ changes in a non-monotonic way. Actually, the latter fact indicates the prevailing role of the impurity energy spectrum change versus the changes of the charge carriers mobility perpendicular to the nanolayers. The constant magnetic field of tension H applied along the normal to clathrate nanolayers GaSe⟨β-CD⟨$FeSO_4$⟩⟩$_Q$ causes the giant magnetoresistance effect (χ = 200…300%) depending on Q (insertion in Fig. 1). In this case, the change of sign $\ln\chi$ causes linking its mechanism with the change of impurity states density asymmetry above and below the Fermi level, which is responsible for the Zeeman localization (delocalization) of charge carriers. This nature is inherent to $La_{0.7}Ba_{0.3}MnO_3$ [15] at room temperature and relatively mild magnetic fields. The important practical value is that the photosensitivity stays at a high level ($\zeta = \rho_{dark}/\rho_{light} = 10^3$) even after the fourfold expansion of the initial matrix GaSe and clathrate formation. As it follows from the insertion in Fig. 1, this parameter increases with increasing Q.

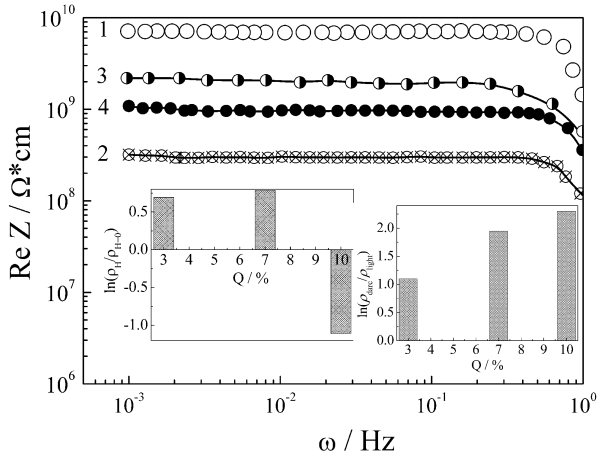

Fig. 1. Infra low-frequency dependences of the real part of the specific impedance that is perpendicular to the layers of GaSe⟨β-CD⟨$FeSO_4$⟩⟩$_Q$ for Q = 3 (*2*), 7 (*3*) and 10 (*4*) mass.%, measured at the temperature 293 K in darkness. (*1*) – extended crystalline matrix. The magnetoresistance (left) and photoresistant (right) effects are shown on the insertions.

The frequency dependences of the imaginary specific complex impedance component GaSe⟨β-CD⟨$FeSO_4$⟩⟩$_Q$ perpendicular to the nanolayers are shown in Fig. 2. It is seen that Im $Z(\omega)$ oscillates not only because of the frequency change, but also it is non-monotonic with regard to Q. Pay attention to the fact that at Q = 7 mass.% its low-frequency region is in IV inductive quadrant of the complex impedance plane. It appears on the Nyquist diagram (Fig. 3, curve *2*) appropriately. This effect, known in the literature as a phenomenon of a "negative" capacity, attracts attention (*e.g.* [16, 17]) due to the possibility of its application in nanoelectronics for creating non-gyrator nanolines delay. We highlighted this issue for semiconductor clathrates of the investigated class in papers [18, 19].

In a magnetic field, the low-frequency inductive response is observed only for Q = 7 mass.% and gains an extraordinary form (Fig. 3, curve *3*), which on the Nyquist chart is shown as a strong instability (bifurcation of the frequency parameter) of Im $Z(\omega)$ in the vicinity of frequency $0.2 < \omega < 0.01$ Hz. In this case, the equivalent electrical scheme corresponds to the branch of the Nyquist hodograph from the vicinity of this frequency, and it is shown in the insertion to Fig. 3.

It's worthy noting that the inductive feedback causes also lighting for this value Q (insertion to Fig. 2).

The synthesized nanohybrids have also interesting polarizing properties. Due to the practical meaning, possibilities of their application for high-quality capacitors in radio-frequency range is now analyzed, the data representing the magnitude of electrical losses tangent of angle less than 1 have been taken into account. The range of frequencies is $10^2 \ldots 10^6$ Hz. In general, variation of the cavitate content β-CD⟨$FeSO_4$⟩ does not cause any significant changes in dielectric susceptibility along the normal to nanolayers of the synthesized supramolecular ensemble in the analyzed frequency range neither in the frequency dependence nor in the magnitude. An exception is for Q = 3 mass.% degree of the guest loading, when a significant reduction of ε at the frequencies up to 10^4 Hz (*e.g.*, the 12-fold one at the frequency close to 1 kHz) is observable.

The imposition of a magnetic field perpendicularly to the nanolayers causes the magnitocapacitance effect, which substantially depends on Q (Fig. 4). A similar situation is realized at illumination. Since the observed changes are conjugated with the abnormal frequency dispersion (growth of ε with increasing the frequency), there are all reasons to consider their nature to be caused by the electronic energy spectrum [20]. In Fig. 4, one can see that in the first case the huge magnitocapacitance positive effect takes place. Its coefficient is $\wp = \dfrac{\varepsilon(H) - \varepsilon(0)}{\varepsilon(0)}$, where $\varepsilon(H)$ and $\varepsilon(0)$ are the dielectric permittivity in a magnetic field and without it, accordingly, at Q = 3 mass.% it is the highest and reaches 53200%. It opens the prospects of replacing the traditional inductive heads used for reading information from magnetic media with the capacitive magnetoelectric elements that allows reducing the size and energy dispersion in them. For comparison, δ_H for $TbMnO_3$ at temperature 3 K and the magnetic field value of 7200 A/m is 10% [21]. Obviously, in this case the HMC mechanism differs from the implemented one in this work. Most likely, this mechanism could be associated with Zeeman modification of the energy spectrum, as it has been successfully made by the authors of [15] for explaining the giant magneto-resistance effect at room temperature in $La_{0.7}Ba_{0.3}MnO_3$.

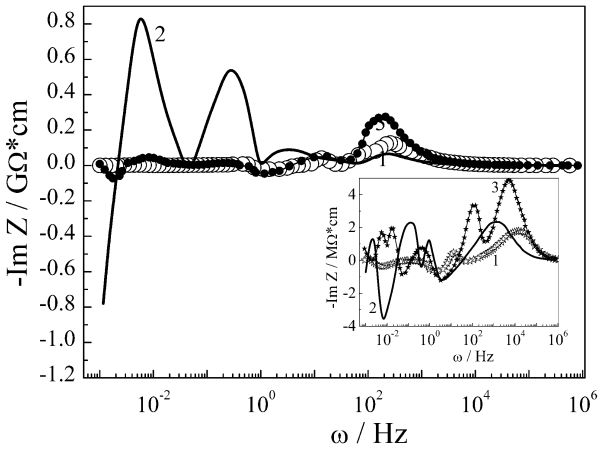

Fig. 2. Frequency dependences of the specific impedance imaginary component perpendicular to the layers GaSe⟨β-CD⟨$FeSO_4$⟩⟩$_Q$ for Q = 3 (*1*), 7 (*2*) and 10 mass.% (*3*), measured under the standard conditions. The measurement results at illumination are shown in the insertion.

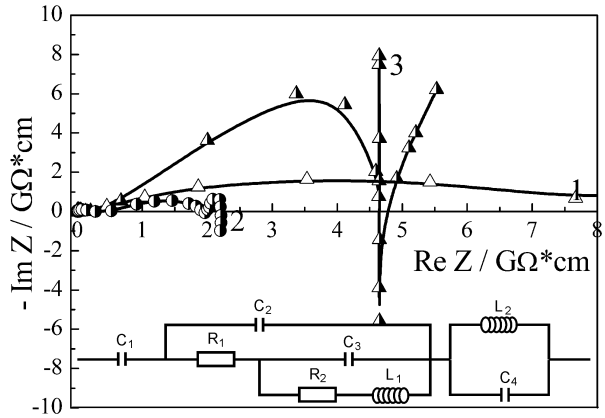

Fig. 3. Nyquist's chart for the direction perpendicular to the nanolayers of the original extended matrix GaSe (*1*) and clathrate GaSe⟨β-CD⟨$FeSO_4$⟩⟩$_{7\ mass.\%}$ for normal conditions (*2*) and magnetic field (*3*). The appropriate equivalent circuits are shown in the insertion.

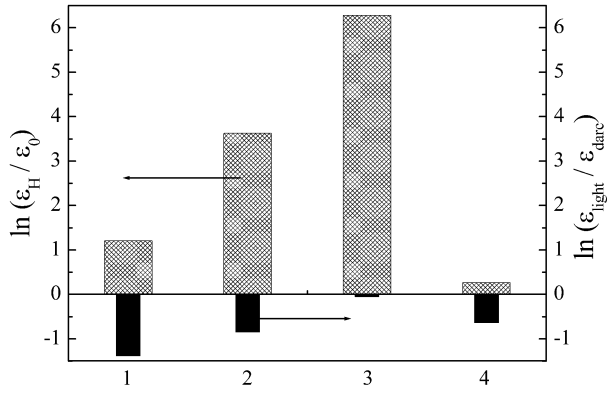

Fig. 4. The dielectric permeability change at frequency 1 MHz in the constant magnetic field and when illuminating GaSe⟨β-CD⟨$FeSO_4$⟩⟩$_Q$ at Q = 3 (*2*), 7 (*3*) and 10 (*4*) mass.%. *1* – primary matrix.

Due to the clathrate principle of the synthesized nanohybrids structure organization with the supramolecular nature of "guest-host" interactions providing the quasi-continuous distribution of the energy states in the band gap of the host material, particularly in the periodic field of coordination defects, it is possible to understand the observed negative photo-dielectric effect, when illuminating with the visible light, because it leads to redistribution of the charge carriers on discrete levels, to polarization of individual centres and changing the density states [22].

As it follows from the parameters shown in Table, the synthesized clathrates of hierarchical architecture GaSe⟨β-CD⟨$FeSO_4$⟩⟩$_Q$ can make the base for hypercapacitant photo and magnetovaricaps of new generation.

The one of the most extraordinary results is a combination of giant magnitude of the dielectric susceptibility and low (less than 1) magnitude of electrical losses tangent of angle in the infra low-frequency region in GaSe⟨β-CD⟨$FeSO_4$⟩⟩$_{Q=7}$. Thus, at $\omega = 10^{-3}$ Hz the value ε is $7 \cdot 10^5$.

Overall, the great importance of the dielectric susceptibility without ferroelectric ordering in the quasi-two-dimensional systems can be grounded as follows.

The one of the possible mechanisms that could explain the described situation is proposed below. The large magnitude of the dielectric susceptibility without segnetoelectric arrangement in quasi-two-dimensional systems can be related with the existence of two-dimensional electron gas (2DEG) in the triangle-like potential well on the border between semiconductor and dielectric. This situation can be described using the model shown in Fig. 5.

The imaginary electrode is the result of charge conservation. The charge of 2DEG should be compensated by the charge on the imaginary electrode. Connection between 2DEG and metallic electrode has a quantum tunnelling nature. This connection causes the levelling of the electrochemical potentials on these electrodes.

Table. Comparative parameters of magneto- and photosensitivity of the capacitive mode at the frequency 500 kHz.

Sample	tg δ	tg δ_H	ε_H	$\varepsilon_H/\varepsilon_0$	tg δ_{light}	ε_{light}	$\varepsilon_{light}/\varepsilon_{dark}$
GaSe⟨β-CD⟨$FeSO_4$⟩⟩$_3$	0.084	0.047	98000	37.5	0.274	1300	0.43
GaSe⟨β-CD⟨$FeSO_4$⟩⟩$_7$	0.006	0.028	9160000	533.0	0.112	18000	1.0
GaSe⟨β-CD⟨$FeSO_4$⟩⟩$_{10}$	0.060	0.084	22000	1.3	0.049	9700	0.5
Yb_2O_3 [23]	0.09	–	–	–	0.12	7.4	2.5–3

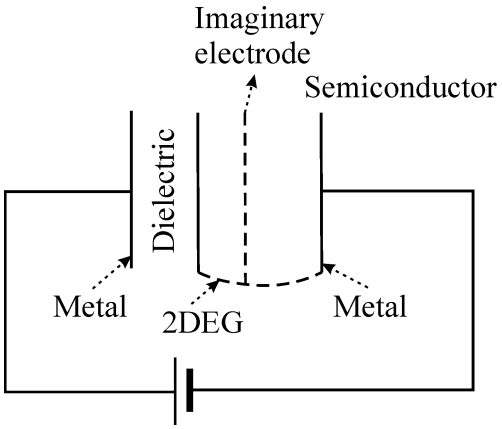

Fig. 5. Equivalent circuit structure.

Let us have charges $+Q$ and $-Q$ on the metallic electrodes. Then, 2DEG-electrode and imaginary electrode will have charges $-q$ and $+q$, accordingly. The magnitude of q depends on the magnitude Q, specifications of the triangle-like potential well and process of tunnelling *etc*.

If we choose the parameters of our electrical circuit as shown in Fig. 6, we will have the following expression for the capacitance of our system

$$C = \frac{S\varepsilon_0}{\frac{1}{2}\left(\frac{D}{\varepsilon_1}+\frac{d_2}{\varepsilon_2}\right)+\frac{q}{2Q}\left(\frac{D}{\varepsilon_1}-\frac{2d_1}{\varepsilon_2}+\frac{d_2}{\varepsilon_2}\right)}$$

Let us accept that $d_1 = d_2 = \frac{d}{2}$ for simplifying our further consideration.

Then, $C = \frac{S\varepsilon_0}{\frac{1}{2}\left(\frac{D}{\varepsilon_1}+\frac{d}{2\varepsilon_2}\right)+\frac{q}{2Q}\left(\frac{D}{\varepsilon_1}-\frac{d}{2\varepsilon_2}\right)}$, and we have three qualitatively different cases:

1. $q = 0$. It means the absence of the 2DEG-electrode. This situation corresponds to the common capacitor with two dielectric layers (D, ε_1) and ($2d$, ε_2).

$$C_{(q=0)} = \frac{2S\varepsilon_0}{\frac{D}{\varepsilon_1}-\frac{d}{2\varepsilon_2}}.$$

2. $q = Q$. This situation is realized when we have ideal connection between metallic electrode and 2DEG-electrode.

$$C_{(q=Q)} = \frac{2S\varepsilon_0\varepsilon_1}{D}.$$

3. $q = \kappa Q$, where κ is a positive number. Let us take $\kappa = 2$ for example. Then,

$$C_{(q=2Q)} = \frac{2S\varepsilon_0}{\frac{3D}{\varepsilon_1}-\frac{d}{2\varepsilon_2}}.$$

In this case, the capacitance of this capacitor becomes larger than the capacitance of a capacitor with the distance between electrodes equal to D. For some κ values, the capacitance can $\to\infty$ and even becomes negative, because we have no restrictions on this κ value. For receiving these restrictions, we should consider a microscopic model of the investigated system. It is important that the proposed model can explain the large magnitude of the capacitance. It is clear that the large magnitude of the capacitance can be related with the large magnitude of effective dielectric susceptibility of the system.

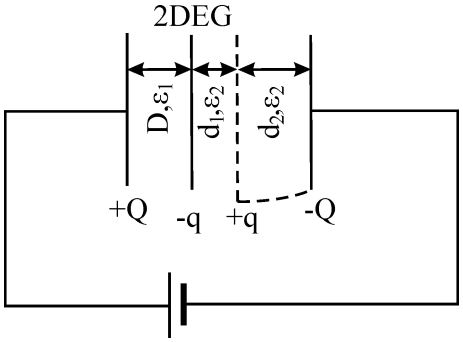

Fig. 6. Parameters of the electric field structure.

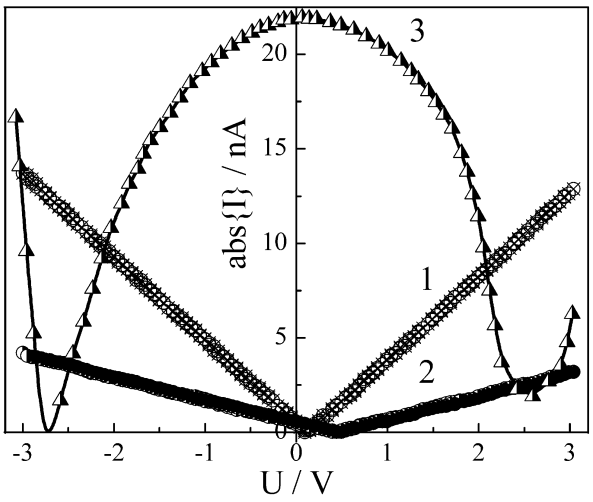

Fig. 7. CVC perpendicular to the layers of GaSe⟨β-CD⟨$FeSO_4$⟩⟩$_Q$ in the magnetic field for Q = 3 (*1*), 7 (*2*) and Q = 10 (*3*) mass.%.

The structure GaSe⟨β-CD⟨$FeSO_4$⟩⟩$_{Q=7}$ is interesting for creating quantum batteries, and, at the same time, clathrate GaSe⟨β-CD⟨$FeSO_4$⟩⟩$_{Q=10}$ promises application in other new direction of the energy storage on the quantum level, the newest alternative to the electrochemical one. In this case, the CVC (Fig. 5) points to observation of the "spin-battery" effect, which value is ~2.6 V at room temperature and the magnetic field close to 2.75 kOe. It is two orders higher than that observed in [24], but at the temperature 3 K and magnetic field 10 kOe. In other words, the hierarchical architecture of 10 mass.% – cavitate loading on the submatrix GaSe is promising for practical implementation of the idea [24] to create a spin capacitor.

It is obvious that the further deepening both experimental and theoretical researches are required to definitly ascertain the nature of the observed phenomena. And these researches are very valuable, as the importance of the proposed approaches to the technology of supersensitive capacitive type sensors of a magnetic field and a field of a light wave at room temperature for developing new approaches to the quantum energy storage is indisputable.

4. Conclusions

1. The doped energy spectrum change is prevailing versus the charge carriers mobility changes perpendicularly to nanolayers with increasing the amount (Q) of guest cavitate β-CD⟨$FeSO_4$⟩ in the expanded van der Waals GaSe regions.

2. The constant magnetic field applied along the normal to clathrate nanolayers GaSe⟨β-CD⟨$FeSO_4$⟩⟩$_Q$ causes a giant magnitoresistance effect, which magnitude and nature depend on Q. However, its photoresistant sensitivity increases with increasing Q.

3. For the guest loading level Q = 7 mass.%, the low-frequency region of imaginary impedance component is in IV inductive quadrant of the complex plane, indicating the possibility of applying the synthesized clathrate in nanoelectronics for creating non-gyrator nanolines delay.

4. In the low-frequency magnetic field, the inductive response is also observed only for Q = 7 mass.%, and on the Nyquist chart it looks like bifurcation on the frequency parameter Im $Z(\omega)$ in the vicinity of the frequencies $0.2 < \omega < 0.01$ Hz.

5. Variation of the cavitate content β-CD⟨$FeSO_4$⟩ does not cause significant changes in $\varepsilon(\omega)$ along the normal to nanolayers in the frequency range $10^2 \ldots 10^6$ Hz. An exception is the guest loading degree Q = 3 mass.%, when significant reduction of ε at frequencies up to 10^4 Hz is observable.

6. The magnetic field application along the perpendicular to the nanolayers causes the magnitocapacitance effect that substantially depends on Q (Fig. 4). A similar situation is realized at the illumination.

7. The huge positive magnetoresistant effect is realized in the magnetic field 2.75 kOe at room temperature. The coefficient of this effect $\wp = \frac{\varepsilon(H) - \varepsilon(0)}{\varepsilon(0)}$, where $\varepsilon(H)$ and $\varepsilon(0)$ are the dielectric susceptibility in a magnetic field and without it, accordingly, is the highest at Q = 3 mass.% and equals to 53200%. It opens the perspective to replace the traditional inductive heads used for reading information from magnetic carriers with the capacitive magnetoelectrical elements, which can reduce the size and the dispersion of energy in them.

8. The synthesized clathrates are promising (especially with the co-intercalation architecture) for new approaches in technology of supersensitive capacitive type sensors of magnetic field and field of light waves at room temperature as well as for creating quantum batteries and spin capacitors, which are the modern alternative to the electrical current chemical sources.

Acknowledgements

This work was partly supported by project №0115U000438 funded by state budget of Ukraine and executed within department theme №0114U001695.temperature range 100…150 K.

The main goal of this work is to obtain TSC spectra for heterostructures InGaAs-GaAs and to interprete them. To reach the goal, the classic method for obtaining TSC spectra and periodic light excitation method during the heating from 83 to 276 K weare used in this paper.

References

1. Slack G.A. *New Materials and Performance Limits for Thermoelectric Cooling, in CRC Handbook of Thermoelectrics*. D.M. Rowe (Eds). CRC Press, Boca Raton, 1995, P. 407−440.
2. Slack G.A., Tritt T.M., Kanatzidis M.G., Lyon H.B., Jr and Mahan G.D. Design concepts for improved thermoelectric materials, *Mat. Res. Soc. Symp. Proc*., Warrendale, Pennsylvania: MRS Press, 1997, pp 47−54.
3. Shevelkov A.V., Kelm E.A., Olenev A.V., Kulbachinskii V.A., Kytin V.G. Anomalously low thermal conductivity and thermoelectric properties of new cationic clathrates in the Sn-In-As-I system. Semiconductors. 2011. **45**. P. 1399−1403.
4. Borshch N.A., Pereslavtseva N.S., Kurganskii S.I. Electronic structure of Zn-substituted germanium clathrates. Semiconductors. 2009. **43**. P. 563−567.
5. Sh. Ibrahim Moustafa, El-din H. Etaiw Safaa, Supramolecular host-guest systems as frameworks for excitation energy transfer. *Spectrochimica Acta*. 2002. **58**. P. 373−378.

6. Bishchaniuk T.M., Grygorchak I.I. Colossal magnetocapacitance effect at room temperature. *Appl. Phys. Lett*. 2014. 104. P. 203104-(1–3).
7. Lies R.M.A. (ed.) *Preparation and Crystal Growth of Materials with Layered Structures.* Dordrecht-Boston, 1977. P. 225−254.
8. Friend R.H., Yoffe A.D. Electronic properties of intercalation complexes of the transition metal dichalcogenides. *Adv. Phys*. 1987. 1. P. 1−94.
9. Chernykh E.V., Brichkin S.B. Supramolecular complexes based on cyclodextrins. High Energy Chemistry. 2010. **44**. P. 83−100.
10. Grygorchak Ivan, Ivashchyshyn Fedir, Stakhira Pavlo, Reghu Renji R., Cherpak Vladyslav, and Grazulevicius Juozas Vidas. Intercalated nanostructure consisting of inorganic receptor and organic ambipolar semiconductor. *J. Nanoelectron. and Optoelectron.* 2013. **8**. P. 292−296.
11. Stoınov Z.B., Grafov B.M., Savova-Stoinova B.S., Elkin V.V. *Electrochemical Impedance.* Nauka, Moscow, 1991, P. 336 (in Russian).
12. *Impedance Spectroscopy, Theory, Experiment and Application*. E. Barsoukov, J.R. Macdonald (Eds.), Wiley Interscience, Canada, 2005, P. 585.
13. Pollak M., Geballe T.H. Low frequency conductivity due to hopping processes in silicon, *Phys. Rev*. 1961. **6**. P. 1743−1753.
14. Olekhnovich N.M., Moroz I.I., Pushkarev A.V., Radyush Yu.V., Salak A.N., Vyshatko N.P., Ferreira V.M. Temperature impedance spectroscopy of $(1-x)Na_{1/2}Bi_{1/2}TiO_{3-x}LaMg_{1/2}Ti_{1/2}O_3$ solid solutions. Physics of the Solid State. 2008. **50**. P. 490−495.
15. Demin R.V., Koroleva L.I., Muminov A.Z., Mukovskii Ya.M. Giant volume magnetostriction and colossal magnetoresistance in $La_{0.7}Ba_{0.3}MnO_3$ at room temperature. Physics of the Solid State. 2006. **48**. P. 322−325.
16. Bisquert J., Randriamahazaka H., Garcia-Belmonte G. Inductive behaviour by charge-transfer and relaxation in solid-state electrochemistry. *Electrochimica Acta*. 2005. 51. P. 627−640.
17. Mora-Sero I., Bisquert J. Implications of the negative capacitance observed at forwards bias in nanocomposite and polycrystalline solar cells. *Nano Lett*. 2006. **6**. P. 640−650.
18. Ivashchyshyn F., Grygorchak I., Stakhira P., Cherpak V., Micov M. Nonorganic semiconductor – Conductive polymer intercalate nanohybrids: Fabrication, properties, application. *Curr. Appl. Phys*. 2012. **12**. P. 160−165.
19. Bishchaniuk T.M., Grygorchak I.I., Fechan A.V., Ivashchyshyn F.O. Semiconductor clathrates with a periodically modulated topology of a host ferroelectric liquid crystal in thermal, magnetic, and light-wave fields. Techn. Phys. 2014. **59**. P. 1085−1087.
20. Žukowski P.V., Partyka J., Wagierek P., Shostak Yu., Sidorenko Yu., Rodzik A. Dielectric properties of $Cd_{1-x}Fe_xSe$ compounds. Semiconductors. 2000. **34**. P. 1124−1127.
21. Kimura T., Goto T., Shintani H., Ishizaka K., Arima T., Tokura Y. Magnetic control of ferroelectric polarization. *Nature*. 2003. **426**. P. 55−58.
22. Anisimova N.I., Bordovskii V.A., Grabko G.I., Castro R.A. Specific features of the photodielectric effect in amorphous As_2Se_3 layers. Techn. Phys. Lett. 2013. **39**. P. 98−100.
23. Rozhkov V.A., Trusova A.Yu. Silicon metal-dielectric-semiconductor varicaps with an yttrium oxide dielectric. Techn. Phys. Lett. 1997. **23**. P. 475−477.
24. Pham Nam Hai, Shinobu Ohya, Masaaki Tanaka, Stewart E. Barnes & Sadamichi Maekawa, Electromotive force and huge magnetoresistance in magnetic tunnel junctions. *Nature*. 2009. **458**. P. 489−493.
25. Supriyo Datta, Proposal for a “spin capacitor”. *Appl. Phys. Lett*. 2005. **83**. P. 013115(1−3).